Proceedings of ASME-JSME-KSME Joint Fluids Engineering Conference 2011
AJK2011-FED
July 24-29, 2011, Hamamatsu, Shizuoka, JAPAN

AJK2011-16026

EXPERIMENTAL INVESTIGATON OF THE SINGLE-PHASE FRICTION FACTOR AND HEAT TRANSFER INSIDE THE HORIZONTAL INTERNALLY MICRO-FIN TUBES IN THE TRANSITION REGION

Hou Kuan Tam
Department of Electromechanical Engineering, Faculty of Science and Technology, University of Macau, Av. Padre Tomás Pereira, Taipa, Macau, China.

Lap Mou Tam
Department of Electromechanical Engineering, Faculty of Science and Technology, University of Macau, Av. Padre Tomás Pereira, Taipa, Macau, China.

Afshin J. Ghajar
School of Mechanical and Aerospace Engineering, Oklahoma State University, Stillwater, Oklahoma, USA.

Cheong Sun
Department of Electromechanical Engineering, Faculty of Science and Technology, University of Macau, Av. Padre Tomás Pereira, Taipa, Macau, China.

Hau Yin Leung
Department of Electromechanical Engineering, Faculty of Science and Technology, University of Macau, Av. Padre Tomás Pereira, Taipa, Macau, China.

ABSTRACT

To increase heat transfer, internally micro-fin tubes are widely used in commercial HVAC applications. It is commonly understood that the micro-fin enhances heat transfer but at the same time increases the pressure drop as well. In the previous studies, majority of the works were focused on the development of correlations in a particular flow regime, especially in the turbulent region. There are only a few works that fundamentally studied the continuous change in the characteristic behavior of pressure drop and heat transfer from laminar to transition and eventually the turbulent regions. Therefore, more in-depth study is necessary. In this study, pressure drop and heat transfer were measured simultaneously in a single test section fitted with several micro-fin tubes and the measured data was compared with the data of a plain tube. There were different fin geometries (fin spiral angle, fin height, and number of fins per cross-sectional area) inside the micro-fin tubes. From the friction factor results, the transition from laminar to turbulent was clearly established and shown to be inlet dependent. The transition friction factor characteristic for the micro-fin tubes was different from that of the plain tube. The transition range for the micro-fin tubes was shown to be much wider than that of the plain tube. From the experimental results, it could also be observed that the increase of fin spiral angle lead to the early transition for the friction factor. For the heating condition, the effect of heating on the friction factor was observed primarily in the lower transition region. From the heat transfer results, the transition from laminar to turbulent was clearly established and shown to be inlet and spiral angle dependent. The larger spiral angle caused the earlier transition and the higher heat transfer inside the micro-fin tube. For all the micro-fin tubes with two inlet types, it can be observed that the efficiency index is larger than one when Reynolds number is larger than 5,000.

Keywords: Friction Factor, heat transfer, transition region, micro-fin tubes

NOMENCLATURE

C_f	fully developed friction factor coefficient (fanning friction factor), $(=\Delta P \cdot D_i/2 \cdot L \cdot \rho \cdot V^2)$,	dimensionless
c_p	specific heat of the test fluid evaluated at T_b,	J/(kg·K)
D_i	inside diameter of the test section (tube),	m
D_o	outside diameter of the test section (tube),	m
e	internal fin height,	mm

h fully developed peripheral heat transfer coefficient, $W/(m^2 \cdot K)$

j Colburn-j factor [$=St\ Pr^{0.67}$], dimensionless

k thermal conductivity evaluated at T_b, $W/(m \cdot K)$

L length of the test section (tube), m

N_s Number of starts/fins inside the cross-section area, dimensionless

Nu local average or fully developed peripheral Nusselt number ($= h \cdot D_i / k$), dimensionless

p axial fin pitch, [$=\pi \cdot D_i / (N_s \cdot \tan \alpha)$], m

Pr local bulk Prandtl number ($=c_p \cdot \mu_b / k$), dimensionless

Re local bulk Reynolds number ($=\rho \cdot V \cdot D_i / \mu_b$), dimensionless

St local average or fully developed peripheral Stanton number [$=Nu/(Pr \cdot Re)$], dimensionless

T_b local bulk temperature of the test fluid, ºC

T_w local inside wall temperature, ºC

V average velocity in the test section, m/s

x local axial distance along the test section from the inlet, m

Greek Symbols

α Spiral angle, degree

η efficiency index, dimensionless

ΔP pressure difference, Pa

μ_b absolute viscosity of the test fluid evaluated at T_b, Pa·s

μ_w absolute viscosity of the test fluid evaluated at T_w, Pa·s

ρ density of the test fluid evaluated at T_b, kg/m^3

Subscripts

plain refers to the plain tube

micro-fin refers to the micro-fin tube

INTRODUCTION

Single-phase liquid flow in internally enhanced tubes is becoming more important in commercial HVAC applications, where enhanced tube bundles are used in flooded evaporators and shell-side condensers to increase heat transfer. This enables water chillers to reach high efficiency, which helps mitigate global warming concerns of HVAC systems. One kind of internally enhanced tube is the micro-fin tube. Jensen and Vlakancic [1] defined the micro-fin tube to have a height less than $0.03D_i$ (i.e. $2e/D_i<0.06$), where D_i is the inside tube diameter and e is the fin height. Basically, such kind of tube is widely used in high flow rate applications because the heat transfer enhancement in high flow rates (turbulent region) is more pronounced than that in the low flow rates (laminar region). Khanpara et al. [2] reported that the turbulent heat transfer in micro-fin tubes had an increase of 30 to 100% with Reynolds numbers between 5,000 and 11,000. Brognaux et al. [3] indicated that there was a 65 to 95% increase in heat transfer for the micro-fin tube over the smooth tube. However, there was also a 35 to 80% increase in the isothermal pressure drop. The work of Jensen and Vlakancic [1] indicated that the micro-fins increased heat transfer ranging from 20 to 220% in the turbulent flow region. However, there was a penalty due to the increase in the friction factor ranging from 40 to 140%. Webb et al. [4] calculated the "efficiency index", defined as the ratio of the heat transfer and the friction factor of enhanced tube to those variables for the plain tube, to vary from 0.98 to 1.18 for the seven different micro-fin tubes with Reynolds numbers between 20,000 and 80,000. For the laminar flow, several researchers [3, 5-7] concluded that the pressure drop and heat transfer were not greatly affected by micro-fins. Trupp and Haine [8] indicated that the secondary flow inside the tube with longitudinal fins was insignificant in the laminar flow and the thermal entry length was shown not to be relevant to the fin geometry.

The tube side roughening increases heat transfer surface area resulting in high efficiency heat exchangers. The increase in the surface area causes low flow rates in the heat exchanger tubes, resulting in the flow to be at Reynolds numbers that are between laminar and turbulent, that is in the transition region. Owing to the high efficiency requirements, it is likely that more HVAC units will operate in the transition region where the understandings of the pressure drop and heat transfer is limited. In the study of Esen et al. [6] the sudden changes in the friction factor and heat transfer with Reynolds number was observed. Different tube size had different onset point of transition. Moreover, the effect of heat transfer on pressure drop is significant within the transition region. However, the end of transition was not evaluated in that study. Also, there was no further discussion on transition region in that study. Jensen and Vlakancic [1] observed that the micro-fin tubes represented a long transitional period in friction factor before becoming fully turbulent at Re $\cong$ 20,000. During the transitional period, the friction factors are insensitive to Reynolds number. Also, this behavior was observed in [3, 5, 9].

According to the plain tube studies done by Ghajar and his coworkers [10-12] the friction factor and heat transfer characteristics, the buoyancy effect, the entry length effect, the start and end of transition, and the effect of heating on friction factor are the important points to be considered in transition flow. However, in the past studies of micro-fin tubes, some of the above-mentioned points were always ignored. Furthermore, the effect of fin geometries on the friction factor and heat transfer in the transition region was also seldom discussed in the past studies. Therefore, the objective of this study is to analyze the friction factor and heat transfer characteristics of the micro-fin tubes in the transition region with the above-mentioned effects taken into consideration.

EXPERIMENTAL SETUP

The pressure drop and heat transfer experimental data used in this study were obtained from the experimental apparatus shown in Figure 1. The local forced and mixed convective heat transfer measurements were made in a horizontal, electrically heated, copper circular straight tube under uniform wall heat flux boundary condition. As shown in Figure 2, two types of inlet configurations (re-entrant and square-edged) were

installed before the test section. A calming and inlet section similar to that used in [10] was used to ensure a uniform velocity distribution at the entrance of the test section. Water and a mixture of water and ethylene glycol were used as the test fluid in the closed-loop experimental system. The DC arc welder provided the uniform heat flux boundary condition to the test section.

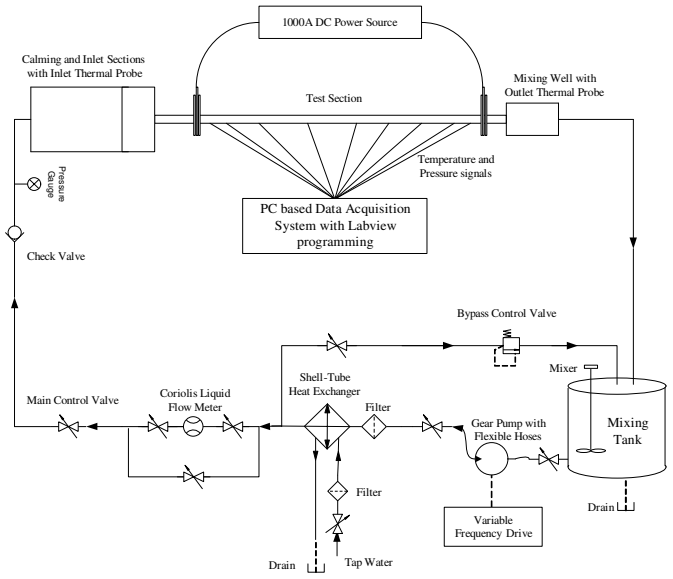

FIGURE 1. EXPERIMENTAL SETUP.

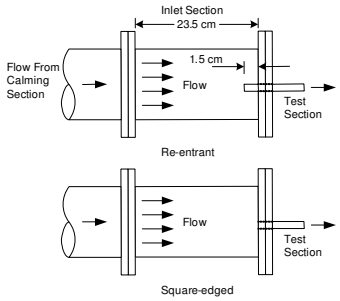

FIGURE 2. TYPE OF INLET.

In this study, the plain tube and micro-fin tubes (see Figure 3) were used as the test section. To study the effect of fin geometries, three micro-fin tubes with different spiral angles were used. Table 1 represents the specification of the tubes. The tubes have an inside diameter of 1.49 cm and an outside diameter of 1.59 cm. The total length of the test section is 6 m, providing a maximum length-to-inside diameter ratio of 403.

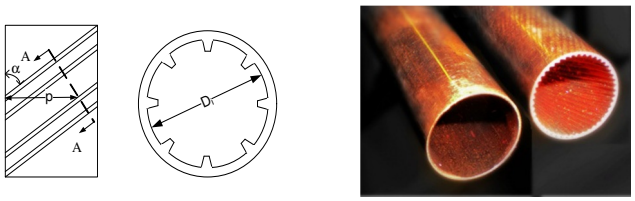

FIGURE 3. (a) SECTIONAL VIEW OF THE MICRO-FIN TUBE; (b) THE PLAIN AND MICRO-FIN TUBES.

TABLE 1. SPECIFICATIONS OF THE TEST TUBES

Tube Type	Outer Dia., D_o (mm)	Inner Dia., D_i (mm)	Spiral angle, α	Fin height, e (mm)	Number of starts, N_s
Plain	15.9	14.9	–	–	–
Micro-fin #1	15.9	14.9	18°	0.5	25
Micro-fin #2	15.9	14.9	25°	0.5	25
Micro-fin #3	15.9	14.9	35°	0.5	25

As shown in Figure 4, the thermocouples denoted as TC1, TC2, TC3, and TC4, were placed 90° apart around the periphery and the single pressure tap was placed between the TC1 and TC2 thermocouples. From the local peripheral wall temperature measurements at each axial location, the inside wall temperatures and the local heat transfer coefficients were calculated by the method shown in [13]. In these calculations, the axial conduction was assumed negligible (RePr > 4,200 in all cases), but peripheral and radial conduction of heat in the tube wall were included. In addition, the bulk fluid temperature was assumed to increase linearly from the inlet to the outlet. Also, the dimensionless numbers, such as Reynolds, Prandtl, Grashof, and Nusselt numbers were computed by the computer program developed by [13]. In the present study, the experiments covered a local bulk Reynolds number range of 1000 to 25000, a local Prandtl number range of 4.8 to 51.9, a local bulk Grashof number range of 1801 to 28619, a local bulk Nusselt number range of 12.4 to 326.9, and a friction factor range of 7.3×10^{-3} to 2.2×10^{-2}. The wall heat flux for the experiments ranged from 3.4 to 6.9kW/m^2.

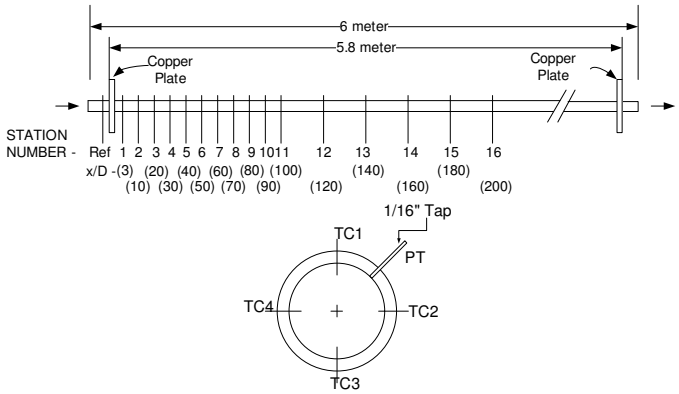

FIGURE 4. ARRANGEMENT OF THE THERMOCOUPLES AND PRESSURE TAP ON THE TEST SECTION.

All the thermocouples and the pressure transducers were calibrated before the experimental runs. The high-precision Coriolis flowmeter was calibrated by the manufacturer. Table 2 lists the uncertainties of the measured variables and calculated variables over the entire range of Reynolds numbers studied. The calculation method is based on Kline and McClintock [14].

TABLE 2. UNCERTAINIES IN EXPERIMENTAL DATA

Measured variables		**Calculated variables**	
Variable	**Uncertainty**	**Variable**	**Uncertainty**
Temperature	0.22 °C	*C_f(friction factor)*	2.1%
Mass flow rate	0.77% of full range (0.3-30USGPM)	*h (heat transfer coefficient)*	12.6%
Density	0.2 kg/m^3	*Nu (Nusselt number)*	12.6%
Diameter	0.02mm		
Length	0.1mm		
Voltage	1%		
Current	1%		

RESULTS AND DISSCUSSION

To verify the new experimental setup and later to compare with the micro-fin tube data, experiments for plain tube were conducted first. The measurements of friction factor were verified by comparing the data collected in this study with the classical friction factor equations for laminar and turbulent flows. As shown in Figure 5, all the recently collected friction factor data matched well (within 10%) with the classical equations for laminar flow (C_f = 16/Re) and turbulent flow (Blasius: $C_f = 0.0791Re^{-0.25}$).

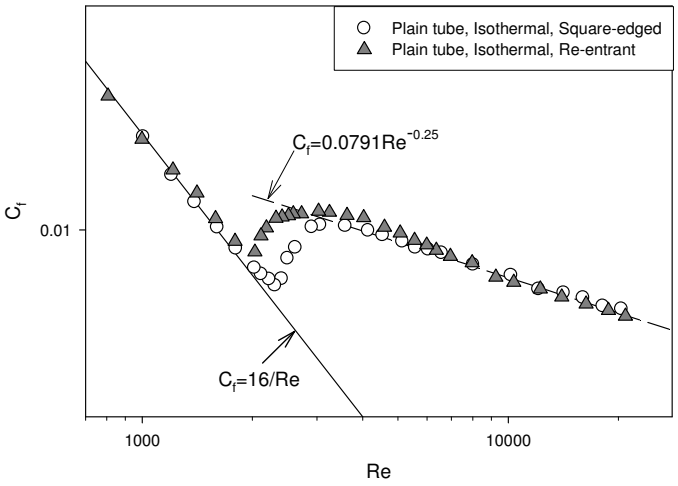

FIGURE 5. FRICTION FACTOR CHARACTERISTICS FOR THE PLAIN TUBE AT x/ D_i OF 200 UNDER ISOTHERMAL BOUNDARY CONDITION.

Figure 6 shows the recently collected plain tube heat transfer data for the square-edged and re-entrant inlets compared with those collected by [10]. Since the deviations between the new data and old data were below 10%, the experimental setup and the data were confirmed to be reliable. It should be noted that the parallel shift from the classical fully developed value of Nu = 4.364 for uniform heat flux boundary condition in the laminar region is due to the buoyancy effect [10].

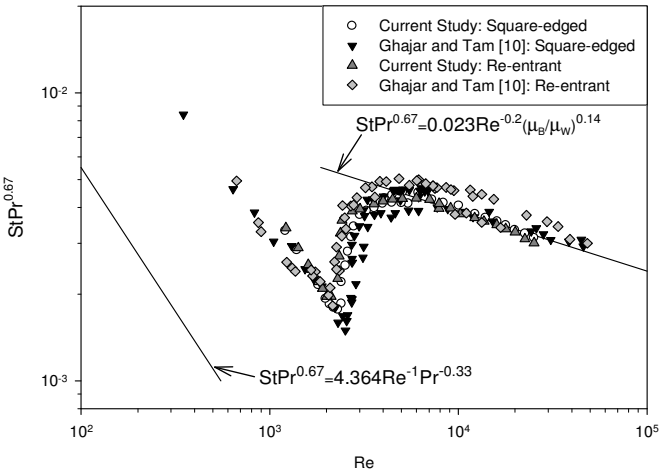

FIGURE 6. HEAT TRANSFER CHARACTERISTICS FOR THE PLAIN TUBE AT x/ D_i OF 200.

TABLE 3. START AND END OF TRANSITION FOR PLAIN AND MICRO-FIN TUBES AT x/ D_i OF 200.

Tube, Condition	**Friction Factor**				**Heat Transfer**			
	Re_{start}	**C_f**	**Re_{end}**	**C_f**	**Re_{start}**	**$StPr^{0.7}$**	**Re_{end}**	**$StPr^{0.7}$**
Plain, Isothermal (Square-edged)	2306	7.6e-3	3588	0.0102	-	-	-	-
Plain, Heating (Square-edged)	2300	7.2e-3	3941	0.0100	2298	1.8e-3	8357	4.1e-3
Plain, Isothermal (Re-entrant)	2032	9.0e-3	3031	0.0110	-	-	-	-
Plain, Heating (Re-entrant)	2001	7.6e-3	3039	0.0106	2001	2.0e-3	7919	4.1e-3
Micro-fin #1, Isothermal (Square-edged)	2675	8.4e-3	8800	0.0144	-	-	-	-
Micro-fin #1, Heating (Square-edged)	2764	7.3e-3	9156	0.0138	2751	1.7e-3	8963	9.4e-3
Micro-fin #1, Isothermal (Re-entrant)	2021	0.0104	8496	0.0143	-	-	-	-
Micro-fin #1, Heating (Re-entrant)	2167	9.2e-3	9027	0.0143	2145	1.9e-3	8014	9.2e-3
Micro-fin #2, Isothermal (Square-edged)	2284	9.9e-3	8359	0.0154	-	-	-	-
Micro-fin #2, Heating (Square-edged)	2390	7.9e-3	8354	0.0155	2402	1.8e-3	8956	0.0106
Micro-fin #2, Isothermal (Re-entrant)	1973	0.0114	8342	0.0154	-	-	-	-
Micro-fin #2, Heating (Re-entrant)	1997	9.8e-3	8278	0.0158	1946	2.2e-3	7791	0.0109
Micro-fin #3, Isothermal (Square-edged)	1962	0.0104	8302	0.0170	-	-	-	-
Micro-fin #3, Heating (Square-edged)	2250	9.6e-3	8050	0.0168	2144	2.0e-3	8051	0.0116
Micro-fin #3, Isothermal (Re-entrant)	1849	0.0119	7989	0.0167	-	-	-	-
Micro-fin #3, Heating (Re-entrant)	1954	0.0110	8106	0.0169	1903	2.3e-3	7170	0.0124

After the verifications of the experimental setup, pressure drop and heat transfer data for the micro-fin tubes were measured simultaneously in a single test section. The results are shown in Figures 7-9 for friction factor and Figure 10 for heat transfer, respectively. As seen in these figures, for plain tube and micro-fin tubes fitted with two type of inlet configurations under isothermal and uniform wall heat flux boundary conditions, the start and end of transition for friction factor and heat transfer were established. The transition Reynolds numbers for friction factor and heat transfer are summarized in Table 3.

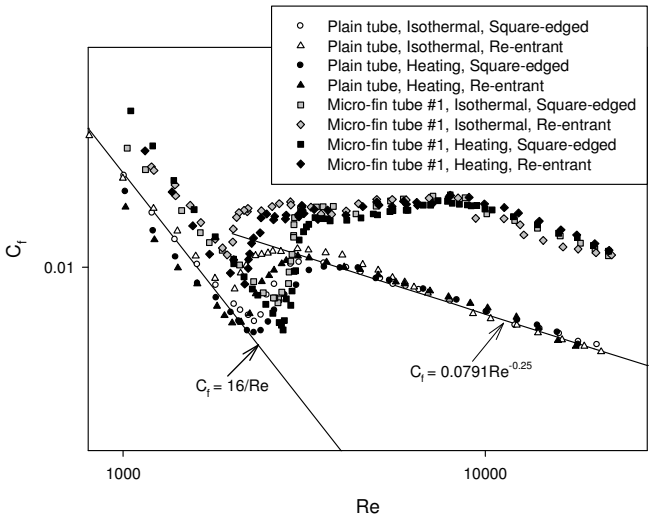

FIGURE 7. FRICTION FACTOR CHARACTERISTICS FOR THE PLAIN TUBE AND THE MICRO-FIN TUBE #1 AT x/ D_i OF 200 UNDER ISOTHERMAL AND HEATING BOUNDARY CONDITIONS.

For the friction factor, as seen in Figure 7, in the laminar region, the friction factor for micro-fin tube #1, either heated or isothermal, exhibits different behavior from the plain tube. For the micro-fin tube a parallel shift from the classical laminar equation was observed. The laminar friction factor for heated or isothermal micro-fin tube has the same trend in the laminar region. In the other words, the friction factor in that region is insensitive to the different boundary conditions. For the isothermal data, the lower transition Reynolds numbers of the micro-fin tube #1 are 2,675 and 2,021 for the square-edged and re-entrant inlets which are different from the plain tube (2,306 and 2,032) and late transition for micro-fin tube is observed. Comparing the isothermal and heated friction factor for micro-fin tube, it can be observed that heating delays the start of transition. As shown in Table 3, the delay of the start of transition is also observed in the other micro-fin tubes. Moreover, as shown in Figure 7, the effect of heating on the micro-fin tube friction factor is mainly present in the lower transition region. In the transition region, the micro-fin tube friction factors go through a steep increase followed by a relatively constant C_f section and then a parallel shift from the classical Blasius turbulent friction factor correlation. The transition range for the micro-fin tubes is shown to be much wider than that of the plain tube. Similar results were also observed in [1, 3, 5, 9]. For the end of the transition for micro-fin tube, it is defined as the first point where the friction factor data becomes parallel to the Blasius correlation. Beyond this point, the flow is considered turbulent.

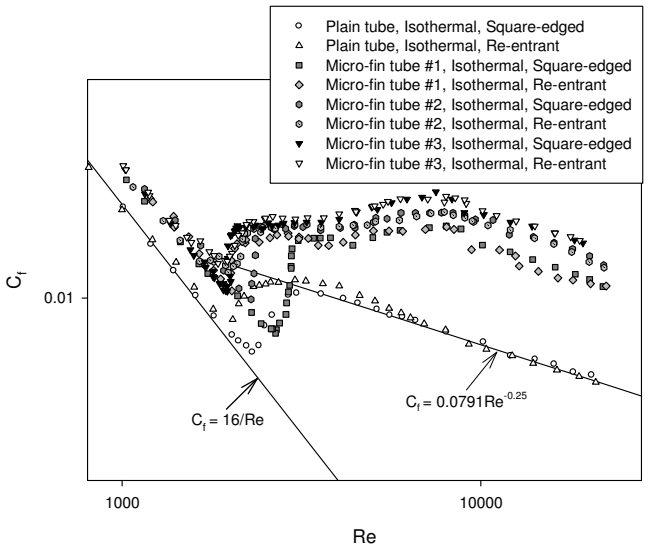

FIGURE 8. FRICTION FACTOR CHARACTERISTICS FOR THE PLAIN TUBE AND THE MICRO-FIN TUBES #1, #2 AND #3 AT x/ D_i OF 200 UNDER ISOTHERMAL BOUNDARY CONDITION.

Figure 8 represents the fully developed friction factor characteristics for the plain and different spiral-angle micro-fin tubes and different inlet configurations under isothermal boundary condition. The parallel shift from the classical laminar equation is also observed in all the micro-fin tubes regardless of the fin geometry and the type of inlets. The laminar friction factor for the isothermal micro-fin tubes has the same trend in the laminar region. In the other words, the friction factor in that region is not only insensitive to the type of inlet, but also insensitive to the fin geometry. For the micro-fin tube #2, the lower transition Reynolds number for the square-edged (Re = 2,284) and re-entrant (Re = 1,973) inlets is different from the micro-fin #1 tube (2,675 and 2,021) and early transition for micro-fin tube #2 with a larger spiral angle is observed. Comparing to the micro-fin tubes #1 and #2, the micro-fin tube #3 with a larger spiral angle has an earlier start of transition (1,962 for square-edged and 1,849 for re-entrant). The micro-fin tube #3 also has an earlier transition when compared to the plain tube. For all the micro-fin tubes, comparing to the re-entrant inlet, it can also be observed that square-edged inlet delays the start of transition. This observation is typically obvious for the micro-fin tube #1 with a smaller spiral angle. In the transition region, the friction factors for all the micro-fin tubes go through a steep increase followed by a relatively constant C_f section and then a parallel shift from the classical Blasius turbulent friction factor correlation. With a higher spiral angle in the micro-fin tube, the increase of friction

factor can be observed in the transition and turbulent regions. The reason is caused by the stronger drag due to the larger spiral angle on the tube wall. As shown in Figure 8 and Table 3, it is also observed that a higher spiral angle in the micro-fin tube advances the end of transition for both inlet configurations.

Figure 9 represents the fully developed friction factor characteristics for the plain and micro-fin tubes with different inlet configurations under heating boundary condition. The parallel shift from the classical laminar equation is also observed in all the micro-fin tubes for both inlets. The laminar friction factor for the heated micro-fin tubes has the same trend in the laminar region. In the other words, the friction factor in that region is also insensitive to the boundary conditions. For the heated data, the lower transition Reynolds numbers of the micro-fin tube #2 (2,390 and 1,997) for the square-edged and re-entrant inlets are different from the micro-fin #1 tube (2,764 and 2,167) and early transition for micro-fin tube #2 with a higher spiral angle is observed. Furthermore, as seen in Table 3, the early transition for micro-fin tube #3 with a larger spiral angle is also observed when compared with the micro-fin tubes #1 and #2. Comparing to the re-entrant inlet, it can also be observed that square-edged inlet delays the start of transition. In the transition region, the heated friction factors for all the micro-fin tubes also go through a steep increase followed by a relatively constant C_f section and then a parallel shift from the classical Blasius turbulent friction factor correlation. With a larger spiral angle in the micro-fin tube, the increase of friction factor can be observed in the transition and turbulent regions. The reason is also caused by the mixing flow near the tube wall. For the heating condition, as shown in Figure 9 and Table 3, it is also observed that the larger spiral angle in the micro-fin tube advances the end of transition.

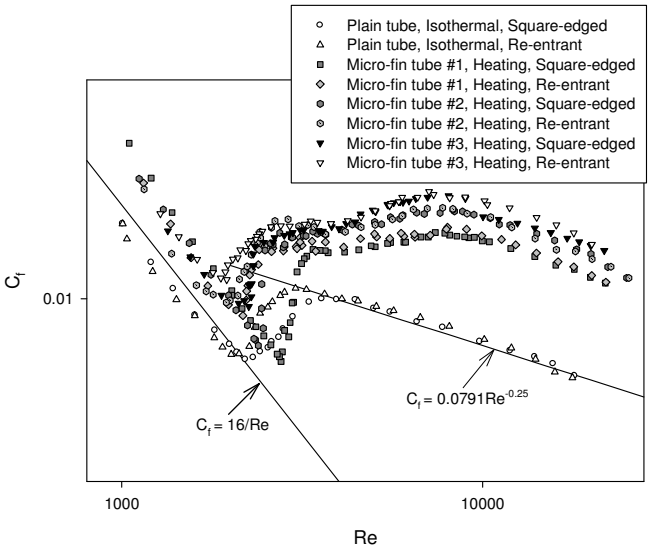

FIGURE 9. FRICTION FACTOR CHARACTERISTICS FOR THE PLAIN AND MICRO-FIN TUBES #1 AND #2 AND #3 AT x/ D_i OF 200 UNDER HEATING BOUNDARY CONDITION.

Regarding to the start and end of transition of heat transfer, it can be observed, in Figure 10, that the start of transition is defined as the critical point for the sudden change from the laminar region (landed on a line parallel to Nu = 4.364) to transition region. For the end of the transition for micro-fin tube, it is defined as the first point where the heat transfer data landed on a line parallel to the correlation proposed by Sieder and Tate [15].

For the heat transfer of micro-fin tube #1 with a spiral angle of 18°, comparing with the plain tube, according to Table 3 and Figure 10, the lower transition is delayed for both square-edged and re-entrant inlets. For the plain tube, the transition Reynolds number for the square-edged and re-entrant is 2298 and 2001, respectively. For micro-fin tube #1, the lower transition Reynolds number increases to 2751 for the square-edged inlet and 2145 for the re-entrant inlet. For the upper transition Reynolds number for tube #1, they are 8963 for the square-edged and 8014 for the re-entrant and therefore, the upper transition is also delayed for both inlet configurations when compared with the plain tube (Re = 8357 for the square-edged inlet and Re = 7919 for the re-entrant inlet).

For the heat transfer of micro-fin tube #2 with a larger spiral angle of 25°, it is observed that the lower transition Reynolds numbers for both square-edged (Re = 2402) and re-entrant (Re = 1946) inlets are advanced when compared with micro-fin tube #1 (Re = 2751 for the square-edged and Re = 2145 for the re-entrant). Comparing to the plain tube, the lower transition Reynolds number for the square-edged is still delayed from 2298 to 2402 but, for the re-entrant, the number is slightly advanced from 2001 to 1946. For the upper transition Reynolds number, the two inlets behaved differently. For the square-edged, the upper transition Reynolds number is almost the same as the micro-fin tube #1. For the re-entrant, the upper transition Reynolds number of the tube #2 is advanced from 8014 to 7791 when compared with the tube #1. Comparing to the plain tube, the upper transition Reynolds number of the tube #2 for the square-edged is delayed from 8357 to 8956 but, for the re-entrant, the upper transition Reynolds number is advanced from 7919 to 7791.

For the heat transfer of micro-fin tube #3 with a much larger spiral angle of 35°, it is observed that the lower transition Reynolds number for both square-edged (Re = 2144) and re-entrant (Re = 1903) inlets is advanced when compared with the micro-fin tube #1 (Re = 2751 for the square-edged and Re = 2145 for the re-entrant) and the micro-fin tube #2 (Re = 2402 for the square-edged and Re = 1946 for the re-entrant). Comparing to the plain tube, the lower transition Reynolds number of the tube #3 for both of the square-edged and the re-entrant is advanced from 2298 to 2144 and from 2001 to 1903. Also, it is also observed that the upper transition Reynolds number (Re = 8051 for the square-edged inlet and Re = 7170 for the re-entrant inlet) is obviously lower than that of the other two micro-fin tubes, tube #1 (Re = 8963 for the square-edged inlet and Re = 8014 for the re-entrant inlet) and tube #2 (Re = 8956 for the square-edged inlet and Re = 7791 for the re-entrant inlet). As comparing with the plain tube, the upper transition

Reynolds number of the tube #3 for the square-edged and re-entrant inlets is advanced from 8357 to 8051 and from 7919 to 7170.

From the above observations, it is obvious that the increase of the spiral angle causes the early transition of heat transfer. It is because the larger spiral angle increases flow disturbance and leads to the earlier transition.

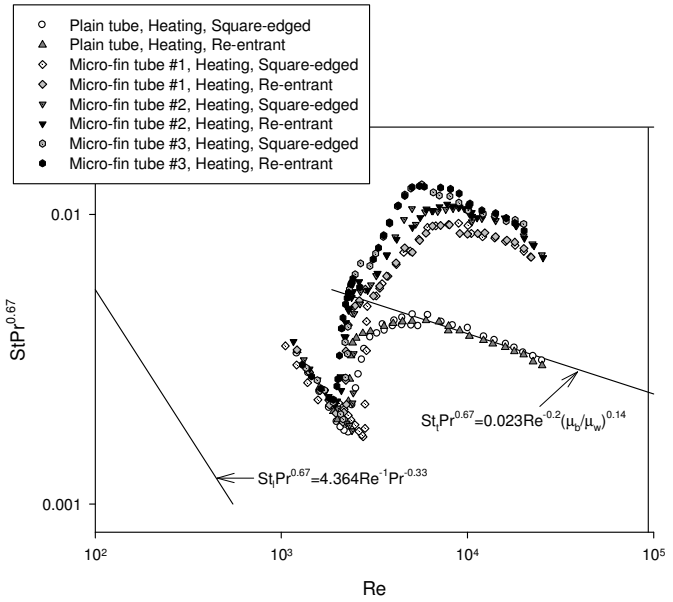

FIGURE 10. HEAT TRANSFER CHARACTERISTICS FOR THE PLAIN AND MICRO-FIN TUBES.

Referring to Figure 10, it is observed that the heat transfer behavior in the upper transition region for the plain and micro-fin tubes is very different. For the plain tube, the heat transfer experienced an abrupt change in the lower transition region and followed by a moderate change in the upper transition and finally the transition ended and the heat transfer data follows the Sieder and Tate correlation [15] at Reynolds number around 8000. However, for the fin tube, such characteristic cannot be seen and the abrupt change was observed in the entire transition region. When Reynolds number is around 8000, a parallel shift of heat transfer data from the Sider and Tate equation was observed. This increase in the Colburn j factor ($St\ Pr^{0.67}$) and the parallel shift from the Sieder and Tate correlation in the turbulent region is due to the swirling motion induced by the micro-fin. The larger spiral angle leads to a higher Colburn j factor. It is because the larger spiral angle increases the fluid mixing between the bulk fluid and the tube wall and therefore the heat transfer is enhanced.

The efficiency index, $\eta = (j/C_f)_{micro-fin}/(j/C_f)_{plain}$ was calculated for the measured Reynolds number range and is plotted in Figure 11. For all the micro-fin tubes with two inlet types. It can be observed that the efficiency index is larger than one when Reynolds number is larger than 5,000. Therefore, it can be concluded that micro-fin tube should not be used in the laminar and even the lower transition regions.

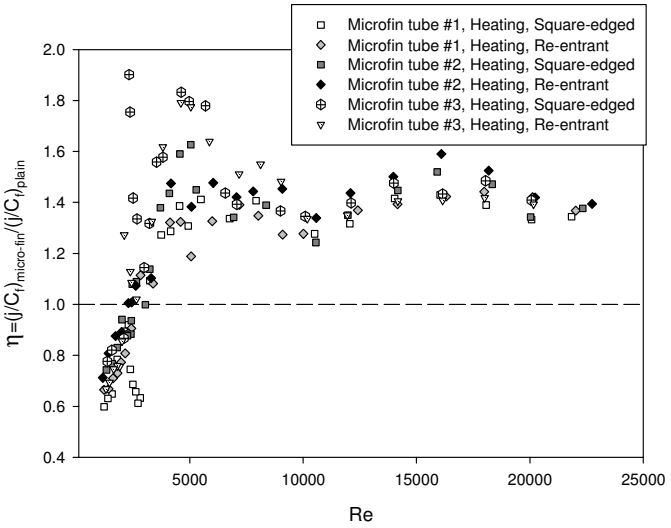

FIGURE 11. EFFICIENCY INDEX.

CONCLUSIONS

In this study, friction factor and heat transfer for horizontal plain and micro-fin tubes were obtained simultaneously under isothermal and uniform wall heat flux boundary conditions. From the results, the transition regions for pressure drop and heat transfer were obtained.

For the micro-fin tube friction factor, a parallel shift in the laminar and turbulent regions was observed. The start and end of transition was inlet dependent and spiral angle dependent. In addition, the transition region for the micro-fin tube friction factor is composed of a steep increase followed by a relatively constant C_f section and the results were comparable with the observations of other researchers. The increase of fin spiral angle leads to the early start and end of transition for friction factor. For the heating condition, the effect of heating on the friction factor was observed primarily in the lower transition region and the heating caused the delay of start of transition.

For the heat transfer, the transition was inlet dependent and the start and end of transition was spiral angle dependent. The delay of transition was obvious for smaller spiral angle while the early transition occurred when larger spiral angle tubes were used. In addition, a parallel shift in the heat transfer data due to the swirling motion induced by the micro-fin was observed in the turbulent region. Therefore, the larger spiral angle caused the early start and end of transition and the higher heat transfer inside the micro-fin tube.

From the friction factor and heat transfer results, it is observed that the larger spiral angle of the micro-fin can increase pressure drop which is caused by the stronger drag due to the larger spiral angle on the tube wall and also enhance the heat transfer due to the occurrence of fluid mixing near the tube wall. In addition, the increase of spiral angle can advance the start of transition. Finally, from the calculated efficiency index values it was concluded that when the Reynolds number is larger than 5,000, regardless of the inlet configuration and fin geometry used, the efficiency index is always greater than 1.

ACKNOWLEDGMENTS

This research is supported by the Fundo para o Desenvolvimento das Ciencias e da Tecnologia under project no. 033/2008/A2 and the Institute for the Development and Quality, Macau.

REFERENCES

[1] Jensen, M. K. and Vlakancic, A., 1999, "Technical note – Experimental investigation of turbulent heat transfer and fluid flow in internally finned tubes", *International Journal of Heat and Mass Transfer*, **42**, pp. 1343-1351.

[2] Khanpara, J. C., Bergles, A. E. and Pate, M. B., 1986, "Augmentation of R-113 in tube evaporation with microfin tubes", *ASHRAE Transactions*, **92**(2b), pp. 506-524.

[3] Brognaux, L. B., Webb, R. L. and Chamra, L. M., 1997, "Single phase heat transfer in micro-fin tubes", *International Journal of Heat and Mass Transfer*, **40**(18), pp. 4345-4357.

[4] Webb, R. L., Narayanamurthy, R. and Thors, P., 2000, "Heat transfer and friction characteristics of internal helical-rib roughness", *Journal of Heat Transfer*, **122**(1), pp. 134-142.

[5] Al-Fahed, S., Chamra, L. M. and Chakroun, W., 1999, "Pressure drop and heat transfer comparison for both microfin tube and twisted tape inserts in laminar flow", *Experimental Thermal and Fluid Science*, **18**, pp. 232-333.

[6] Esen, E. B., Obot, N. T. and Rabas, T. J., 1994, "Enhancement: Part I. Heat transfer and pressure drop results for air flow through passages with spirally-shaped roughness", *Journal of Enhanced Heat Transfer*, **1**(2), pp. 145-156.

[7] Shome, B. and Jensen, M. K., 1996, "Experimental investigation of laminar flow and heat transfer in internally finned tubes", *Journal of Enhanced Heat Transfer*, **4**(1), pp. 53-70.

[8] Trupp, A. C. and Haine, H., 1989, "Experimental investigation of turbulent mixed convection in horizontal tubes with longitudinal internal fins", *National Heat Transfer Conference*, *Philadelphia*, *PA*, HTD-**107**, Heat Transfer in Convective Flows, pp. 17-25.

[9] Chiou, C. B., Wang, C. C. and Lu, D. C., 1995, "Single phase heat transfer and pressure drop characteristics of microfin tubes", *ASHRAE Transactions*, **101**(2), pp. 1041-1048.

[10] Ghajar, A. J. and Tam, L. M., 1994, "Heat transfer measurements and correlations in the transition region for a circular tube with three different inlet configurations", *Experimental Thermal and Fluid Science*, **8**(1), pp. 79-90.

[11] Tam, L. M. and Ghajar, A. J., 1997, "Effect of inlet geometry and heating on the fully developed friction factor in the transition region of a horizontal tube", *Experimental Thermal and Fluid Science*, **15**(1), pp. 52-64.

[12] Tam, L. M. and Ghajar, A. J., 2006, "Transitional Heat Transfer in Plain Horizontal Tubes," *Heat Transfer Engineering*, **27**(5), pp 23-38.

[13] Ghajar, A. J. and Kim, J., 2006, *Heat Transfer Calculation*s (edited by Myer Kutz), *Calculation of local inside-wall convective heat transfer parameters from measurements of the local outside-wall temperatures along an electrically heated circular tube*, McGraw-Hill, New York, NY, pp. 23.3-23.27.

[14] Kline, S. J. and McClintock, F. A., 1953, "Describing Uncertainties in Single Sample Experiments," *Mech. Eng.*, **75**(1), pp. 3-8.

[15] Sieder, E. N. and Tate, G. E., 1936, "Heat Transfer and Pressure Drop in Liquids in Tubes," *Ind. Eng. Chem.*, **28**, pp. 1429-1435.